Clim. Past, 8, 205–213, 2012
www.clim-past.net/8/205/2012/
doi:10.5194/cp-8-205-2012

Reconstruction of southeast Tibetan Plateau summer climate using tree ring δ^{18}O: moisture variability over the past two centuries

C. Shi[1,2,6], V. Daux[2], Q.-B. Zhang[1], C. Risi[3], S.-G. Hou[4], M. Stievenard[2], M. Pierre[2], Z. Li[5], and V. Masson-Delmotte[2]

[1]State Key Laboratory of Vegetation and Environmental Change, Institute of Botany, Chinese Academy of Sciences, Beijing 100093, China
[2]Laboratoire des Sciences du Climat et de l'Environnement, UMR8212, IPSL/CEA/CNRS/UVSQ Bat 701, L'Orme des Merisiers, CEA Saclay, 91 191 Gif sur Yvette Cedex, France
[3]CIRES, University of Colorado, 80309 Boulder CO, USA
[4]Key Laboratory for Coast and Island Development, Ministry of Education, School of Geographic and Oceanographic Sciences, Nanjing University, 22 Hankou Road, Nanjing 210093, China
[5]Research center For Eco-Environment Change, Chinese Academy of Sciences, Beijing 100085, China
[6]Graduate School of Chinese Academy of Sciences, Beijing 100049, China

Correspondence to: Q.-B. Zhang (qbzhang@ibcas.ac.cn)

Received: 4 April 2011 – Published in Clim. Past Discuss.: 9 June 2011
Revised: 2 December 2011 – Accepted: 7 December 2011 – Published: 2 February 2012

Abstract. A tree-ring δ^{18}O chronology of Linzhi spruce, spanning from AD 1781 to 2005, was developed in Bomi, Southeast Tibetan Plateau (TP). During the period with instrumental data (AD 1961–2005), this record is strongly correlated with regional CRU (Climate Research Unit) summer cloud data, which is supported by a precipitation δ^{18}O simulation conducted with the isotope-enabled atmospheric general circulation model LMDZiso. A reconstruction of a regional summer cloud index, based upon the empirical relationship between cloud and diurnal temperature range, was therefore achieved. This index reflects regional moisture variability in the past 225 yr. The climate appears drier and more stable in the 20th century than previously. The drying trend in late 19th century of our reconstruction is consistent with a decrease in the TP glacier accumulation recorded in ice cores. An exceptional dry decade is documented in the 1810s, possibly related to the impact of repeated volcanic eruptions on monsoon flow.

1 Introduction

Clouds formed by condensation of atmospheric moisture release latent heat in the atmosphere and can scatter, absorb and reflect radiative fluxes. Through their impacts on the atmosphere and surface energy budgets, they play a crucial role in the climate system (Yu et al., 2004; Stephens, 2005). Cloud feedbacks are particularly important in the response of the climate system to radiative perturbations (Dufresne and Bony, 2008). Regional cloud cover is also sensitive to atmospheric aerosol load, which is strongly affected by volcanic eruptions (Robock, 2000) and human activities (Khain et al., 2005; You et al., 2010), with potential positive feedbacks (Jacobson, 2001; Ramanathan et al., 2005).

On the Tibetan Plateau (TP), a significant increase in low clouds has been shown on the eastern TP since the 1980s (You et al., 2010), as well as a decreased cloud variability (Zhang et al., 2008). An increase in night cloud cover (Duan and Wu, 2006), which has amplified the fast regional warming on the TP (Duan and Wu, 2006; Wang et al., 2008), is also reported. Because of the important role of cloud cover in climate dynamics, it is crucial to place the recent changes in the context of a longer time scale to understand the full spectrum of cloud cover variability beyond the short instrumental records and to investigate whether these changes exceed the natural cloud cover variability.

Cloud cover is negatively correlated with diurnal temperature range and sunshine duration and positively correlated with precipitation and summer relative humidity at both regional and global scales (Karl et al., 1993; Dai et al., 1997; Leathers et al., 1998; Trigo et al., 2002; Auer et al., 2007; in the Qinghai-Tibet plateau: Zhang et al., 2008) and at individual weather stations (Wang et al., 1993; Ruschy et al., 1991). Correlations between tree-ring cellulose δ^{18}O and both cloud cover and sunshine duration have been reported. They were attributed to the close relationships between cloudiness and key factors controlling cellulose δ^{18}O, such as precipitation and humidity (Hilasvuori and Berninger, 2010; Kress et al., 2010).

We have recently measured tree-ring cellulose δ^{18}O in Bomi (southeast TP, 95.55° E, 29.87° N) and examined its correlations with local and regional climatic parameters during the instrumental period (Shi et al., 2011). The Bomi tree-ring δ^{18}O is significantly correlated with local and regional CRU cloud cover data (New et al., 1999, 2000). These gridded data were constructed using a combination of observed data and empirical relationships with TP diurnal temperature range (Mitchell and Jones, 2005). The strongest squared correlation coefficient ($r^2 = 0.40$, $p < 0.01$, AD 1956–2005) is observed between Bomi tree-ring δ^{18}O and June–August regional CRU cloud data, upstream of Bomi (28–31° N 90–95° E). This shows the potential of longer tree-ring δ^{18}O records to reconstruct past variations of the regional cloudiness and moisture variability.

Compared to other tree-ring proxies, tree-ring δ^{18}O has several advantages: (i) little evidence of age effects (Masson-Delmotte et al., 2005; Etien et al., 2008; Liu et al., 2008; Shi et al., 2011; Young et al., 2011); (ii) strong and stable correlations with moisture parameters, which are largely influenced by relative humidity (Barbour, 2007; Sternberg, 2009); and (iii) the ability to document past climate variability in moist and warm areas, where no clear factor is limiting tree growth (Evans and Schrag, 2004; Managave et al., 2010; Sano et al., 2010).

In this manuscript, we extend the Bomi tree-ring cellulose δ^{18}O record back to AD 1780 and reconstruct a summer regional cloud index for the past 225 yr. The variability of this reconstruction is analysed in terms of trends, regime shifts and frequency of extreme years. Our reconstruction is also compared with past snow accumulation and δ^{18}O derived from ice cores.

2 Material and method

2.1 Sampling site and strategy

Our tree-ring sampling was conducted in Gangcun Natural Forest Reserve (95.55° E, 29.87° N, ca. 2760 m), which is located 20 km west of Bomi city and 60 km from the turning point of Yaluzangbo-Brahmaputra River (Fig. 1). The forest is well protected and does not exhibit any sign of anthropogenic influence. The main species of this forest are Linzhi spruce (*Picea likiangensis var. lintziensis*) and East Himalayan Fir (*Abies spectabilis*). Linzhi spruce is a shallow rooted and shade tolerant species, mainly distributed within moist areas of southeast TP. We selected 27 Linzhi spruce trees that have no distorted stem or internal rot for sampling. One core per tree was collected at breast height, using an increment borer of 5.14 mm inner diameter. The length of

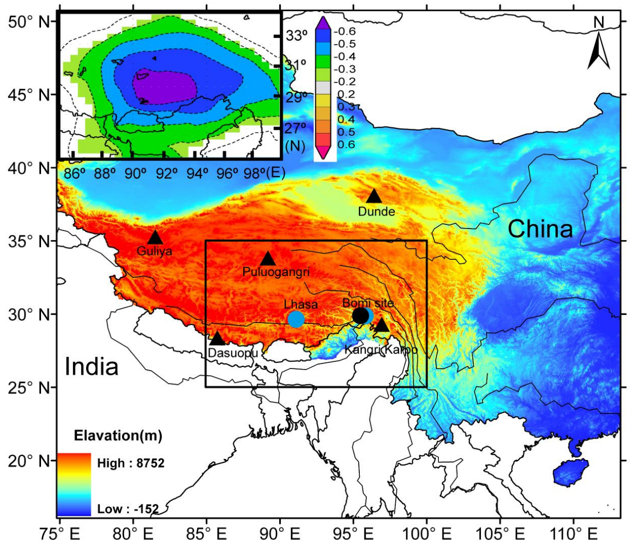

Fig. 1. Map of the study area and location of sites: tree ring sampling site (black circles), Bomi and Lhasa meteorological stations (blue circles), glacier ice core drilling sites (black triangles). The shading depicts the local topography. The subplot in the top-left corner shows the inter-annual correlation coefficients between Bomi tree-ring cellulose δ^{18}O and the regional CRU cloud data (25° N–35° N 85° E–100° E, rectangular in the map); contours are displayed for increments of the correlation coefficients ($p < 0.05$, $n = 46$). The cloud data were obtained from CRU version 2.0 (New et al., 1999, 2000).

cores ranges from 30 cm to 55 cm and most cores reach the pith of the tree.

2.2 Sample preparation and crossdating

Cores were air dried and polished with progressively finer sandpaper until rings were clearly visible. Tree-ring widths (TRW) were measured using the videoment® system and cross-dated by visual inspection of the ring-width pattern. A total of 26 cores were successfully cross-dated and the dating quality was checked using the COFECHA software (Holmes, 1998).

2.3 Tree-ring δ^{18}O measurement

Among the successfully cross-dated cores, 11 old ones (labelled O1 to O11 following age ascendant order) having regular ring boundaries and no missing rings, were chosen for tree-ring δ^{18}O analyses. Each ring of each core was cut using a scalpel blade and stored in an individual plastic tube. For the time period 1956–2005, individual tree-ring δ^{18}O measurements were conducted on five trees and compared to the value obtained on the pooled six other trees. The average of the individual measurements and the pooled result are highly correlated ($r = 0.90$, $p < 0.01$) with no difference in mean level (Shi et al., 2011). We had previously shown that four trees with one core per tree were sufficient to represent a population signal, and that no age effect was found for this species (Shi et al., 2011). We therefore pooled all the tree-ring samples prior to AD 1956 before conducting the cellulose δ^{18}O measurements.

Each wood sample was milled, and alpha cellulose was extracted by chemical extraction, following the procedure described in Raffalli-Delerce et al. (2004). Samples of 0.1–0.2 mg of cellulose were packed in silver capsules and δ^{18}O was measured with a high temperature analyzer (TC/EA) coupled with a Finnigan MAT252 mass spectrometer at LSCE (Gif/Yvette of France) (Shi et al., 2011). The δ^{18}O measurements were conducted with reference to CC31 cellulose standards (31.85 ‰), and the standard deviations of 10 consecutive CC31 (0 to 2 values being rejected) was controlled to be lower than 0.20 ‰. Each sample was measured at least twice, and up to four times if the cellulose amount was sufficient. The analytical uncertainty is 0.2 ‰ (maximum accepted standard deviation on the mean).

3 Results

3.1 Tree-ring δ^{18}O chronology

The tree-ring δ^{18}O and analytical uncertainties are displayed in Fig. 2a, together with the number of trees pooled for δ^{18}O analysis.

3.2 Calibration and verification of the tree-ring δ^{18}O in relation to CRU cloud data

Our previous calibration study (Shi et al., 2011) revealed a significant correlation with regional June-August CRU cloud data, which is based upon the empirical relationship between diurnal temperature range and cloud cover ($r^2 = 0.40$, $n = 46$, $p < 0.01$). This correlation can be explained by several mechanisms. First, cloud cover is correlated with other surface climate factors such as relative humidity and precipitation ($r = 0.46$ $p < 0.01$; $r = 0.35$ $p < 0.05$ for humidity and precipitation respectively), directly affecting tree physiology. Second, cloud cover is likely related to inter-annual variations in monsoon flow and precipitation amount, themselves related to surface vapour and precipitation δ^{18}O, through the amount effect demonstrated at Bomi at the event base (Jing et al., 2011). We will investigate this last point in Sect. 4.1 using atmospheric model results.

Two outlier years, AD 1978 and AD 1991, are detected (Fig. 3, blue arrows). The δ^{18}O measurements of AD 1978 did not yield reproducible results, as six replicates failed to produce a reliable mean value (SD = 0.5 ‰, which extends beyond our accepted threshold of 0.2 ‰). When ignoring this outlier year, 50 % variance of tree-ring δ^{18}O is explained by the variability of June–August CRU cloud data ($n = 45$, $p < 0.01$) (Fig. 3). The linear calibration equation relating June–August CRU cloud cover data (CC_{JJA}, expressed in %) with tree ring cellulose δ^{18}O (in ‰) is:

$$CC_{JJA} = -1.45 \times \delta^{18}O + 116 \quad (1)$$

Leave-one-out cross verification was conducted. RE (reduction of error statistic) and CE (coefficient of efficiency) are both equal to 0.44, which means that the linear calibration is valid. We therefore propose to estimate, prior to the instrumental period, a reconstructed cloud cover index, from this calibration with CRU cloud cover data. We chose to use the term "cloud index" to highlight the fact that (i) our calibration is not performed with direct cloud observations, but with the CRU product based on meteorological data scaled to a short cloud observational record; and (ii) our tree ring data are sensitive to a variety of moisture indicators (precipitation, relative humidity, etc.) in addition to the strongest linear relationship with CRU cloud data (Shi et al., 2011).

The uncertainty on the reconstructed cloud index arises from the uncertainty associated with the linear model and from the uncertainty on the δ^{18}O measurements (on average ± 0.20 ‰). The uncertainty associated with the linear model was estimated using a bootstrap method. Two thirds of the data (calibration samples) were randomly sampled with replacement; the best multiple linear regression was calculated on these data and the quality of the reconstruction was assessed on the last third of the data (verification samples). Further uncertainties on the reconstructed CC_{JJA} may arise from the uncertainty on the proxy measurements. Our analytical protocol warrants an uncertainty on each annual δ^{18}O measurement within ± 0.2 ‰; we have used the bootstrap method to test the quality of the linear regression model, taking into account these uncertainties on the proxies by randomly modifying the proxy data within their uncertainty range. In this case, the standard deviation of the residuals obtained over verification sub-datasets was ± 1.48 % (1000 iterations). Therefore, in order to have a conservative estimate of the quality of the reconstruction, we consider the error on the reconstructed CC_{JJA} to be ± 2.2 ($1.5\,\sigma$).

3.3 Reconstruction of past cloud cover variability

The past variability of the regional cloud index (28–31° N, 90–95° E) was reconstructed by applying Eq. (1) to the 225-yr long chronology of tree-ring δ^{18}O (Fig. 2b). The long-term variability of the cloud index reconstruction was analysed using 30 yr Gaussian low-pass filter. To test the mean value shift of our cloud index reconstruction, a regime shift analysis was conducted with software Regime Shift Detection v3.2 (Rodionov, 2004). The long-term trend is shown in Fig. 2b, and three major shifts in years AD 1807, AD 1818 and AD 1887 are found. From the 1780s to the 1880s, the reconstructed CC_{JJA} shows a plateau of relatively high values, interrupted by an 11-yr sharp minimum (from AD 1807 to 1817). A downward trend is observed from the 1870s to the 1890s, followed by small fluctuations around stable mean

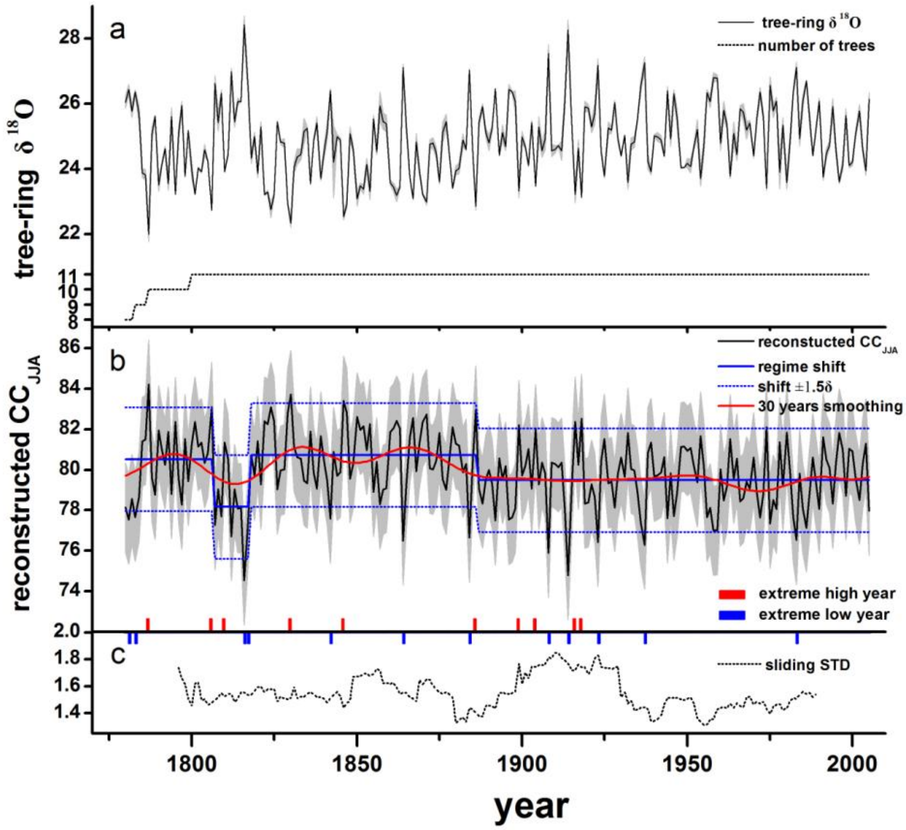

Fig. 2. Panel **(a)**: tree-ring δ^{18}O with measurement uncertainty (grey shading) and number of pooled trees. Panel **(b)**: reconstructed cloud cover (CC) and regime shift. The black line is the reconstructed CC_{JJA}, with its uncertainty depicted in grey shading ($1.5\,\sigma$), the solid blue line is the regime shifts (window length =15 yr, confident at 95 %); the thick red line is 30 yr Gaussian low-pass filter of the reconstructed CC_{JJA}; the red and blue bars correspond to extreme high/low cloud cover years (exceeding 1.5 standard deviations at the base of regime). Panel **(c)**: 31 yr moving standard deviation (STD) of the CC_{JJA} residual (calculated as the difference between the reconstructed CC_{JJA} and its mean baseline, shown by the solid blue line in panel **b**).

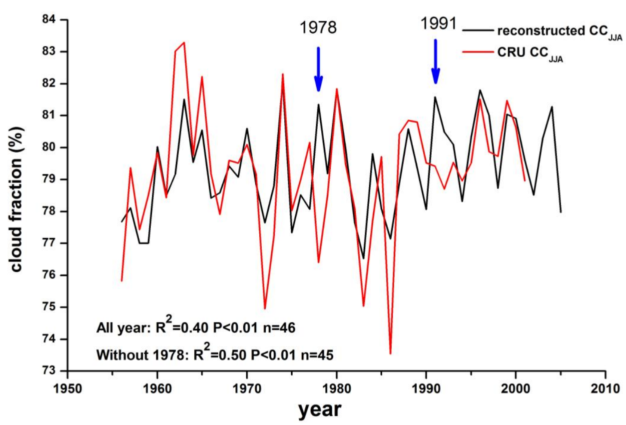

Fig. 3. Reconstructed and CRU June–August cloud covers (CC_{JJA}) over 1956–2005. The black and red lines are reconstructed and CRU cloud respectively. The blue arrows indicate the outlier years of 1978 and 1991.

values. The recent increasing trend is not unprecedented and appears small in comparison to past regime shifts.

To depict the inter-annual variability, we investigated extreme years with high/low cloud index, as well as the moving standard deviation (STD) of the residual record (yearly cloud index minus the mean regime). The extreme years are defined as those with a reconstructed residual cloud index exceeding 1.5 standard deviation from the base level (dashed blue lines in Fig. 2b), and represented with red and blue vertical bars, respectively (Fig. 2b). From the 1920s onwards, few extreme years are evidenced and the variability of the 31-yr moving STD is low (Fig. 2c). The inter-annual to decadal variability of the reconstructed cloud index appears to have been maximum in the years AD 1900–1930, and about 25 % higher than during the last 50 yr (Fig. 2c).

4 Discussion

4.1 Analysis of atmospheric simulations

The oxygen isotopic compositions of regional precipitation and vapour were simulated using the isotope-enabled general circulation model LMDZ (Hourdin et al., 2006), nudged by atmospheric reanalyses over the AD 1981–2007 period after 3 yr of spin-up (Gao et al., 2010; Risi et al., 2010). The simulated summer precipitation and vapour δ^{18}O at Bomi are significantly anti-correlated with the simulated summer regional (25° N–35° N, 85° E–100° E) cloud water content and low cloud cover ($r = -0.41$, $p < 0.05$ in both cases). Spatially, correlation is maximum with cloud water content upstream the air mass trajectories. In the model, this anti-correlation mostly results from the amount effect, with an anti-correlation between precipitation δ^{18}O and regional precipitation amount, itself closely linked with the regional low cloud cover and cloud water content. Cellulose δ^{18}O therefore appears related to cloud cover through the link with the precipitation δ^{18}O, and possibly (albeit not quantitatively investigated) through leaf water enrichment effects (Shi et al., 2010).

We therefore conclude that the most likely explanation for the Bomi cellulose δ^{18}O variability is a simultaneous variability in regional cloud cover associated with changes in upstream monsoon flow, which also correlates with changes in Bomi surface air relative humidity. This is consistent with several tree-ring ecophysiological studies showing that relative humidity is the major driving force of cellulose δ^{18}O (Roden and Ehleringer, 2000; Helliker and Richter, 2008; Sternberg, 2009).

4.2 The 1807–1817 anomaly

In this section, we focus on the regime shift observed from AD 1807 to 1817. This period is characterized by the lowest cloud index. According to large-scale tree-ring based temperature reconstructions, the 1810s is the coldest decade of the past 250 yr to 600 yr in the Northern Hemisphere (Briffa et al., 1998, 2001; Briffa and Osborn, 1999; Esper et al., 2002). This cold event was reported in many Asian areas, including Sichuan (Bräuning and Mantwill, 2004; Song et al., 2007) and Northwest Yunan (Fan et al., 2008), two Chinese provinces adjacent to the TP. A cold anomaly was also evidenced in southeast TP (150 km southwest of our site) in a TRW-based summer temperature reconstruction, which showed the 1810s–1820s as the coldest period in the last 242 yr (ca. 0.5 °C below the mean) (Liang et al., 2009). The climate anomaly of the 1810s was attributed to two consecutive volcanic eruptions: a large tropical eruption of unknown origin, which occurred near the beginning of AD 1809 (Dai et al., 1991; Cole-Dai et al., 2009; Dai, 2010); followed by the AD 1815 eruption of the Indonesian Tambora Volcano (Briffa et al., 1998). Several General Circulation Models (GCMs) predict that large volcanic eruptions should also result in anomalous dry conditions throughout much of monsoon Asia (Oman et al., 2005; Schneider et al., 2009; Fan et al., 2009). Indeed, in the Yunnan province during the AD 1815–1817 interval, serious deficiencies in the monsoon rainfall led to crop failures and to the worst starvation recorded in documented history (Yang et al., 2005). In contrast with modelling and historical sources, at the grid points closest to Bomi, the Palmer Drough Severity Indices reconstructions of the Monsoon Asia Drought Atlas show a moderately dry, almost normal 1810s decade (Cook et al., 2010; Anchukaitis et al., 2010).

If Bomi cellulose δ^{18}O was temperature driven, colder conditions would induce a δ^{18}O drop, in contrast with our data. Today, the cellulose δ^{18}O is mainly controlled by amount effects (via the δ^{18}O of the precipitation) and evaporative enrichment (in direct connection with local humidity). A weakening of the monsoon, which would lead to a decrease of cloud cover, precipitation and relative humidity, would be consistent with the observed increase of cellulose δ^{18}O (decreased rainfall resulting in an increase of precipitation δ^{18}O, combined with decreased evaporative enrichment).

In order to assess if the Bomi signal is associated with a widespread precipitation isotopic composition anomaly, we have compared our record with published ice-core δ^{18}O from Dunde, Dasuopu and Guliya drilling sites, albeit not located upstream or downstream of the monsoon flow to Bomi (only decadal averaged data are available) (Thompson et al., 1989, 1997, 2000) (Fig. 4). There is no ice core evidence for a positive isotopic anomaly in precipitation in the 1810s.

We conclude that the sharp tree ring cellulose anomaly detected in Bomi tree-ring cellulose δ^{18}O in the 1810s is likely caused by a reduced local monsoon flow, and drier conditions of exceptional decadal duration, possibly related with the regional impacts of repeated volcanic eruptions.

4.3 Southeast Tibetan Plateau drying in the late 19th century

The Bomi data show a significant regime shift in the late 19th century towards drier conditions. Other moisture records are available to assess if this is a local or a more widespread signal.

Yao et al. (2008) reconstructed past annual precipitation accumulation using four TP ice cores (Dasuopu, Dunde, Guliya, Puruogangri). Dunde, Guliya and Puruogangri Glacier all depict a dramatic decreased accumulation at the end of the 19th century (Yao et al., 2008), consistent with a reduced low-level jet since the late 19th century in the Indian Ocean (Gong and Luterbacher, 2008). These results support our interpretation of the 1890s regime shift detected in the Bomi tree-ring δ^{18}O in terms of TP moisture availability. The cause for this shift remains to be investigated.

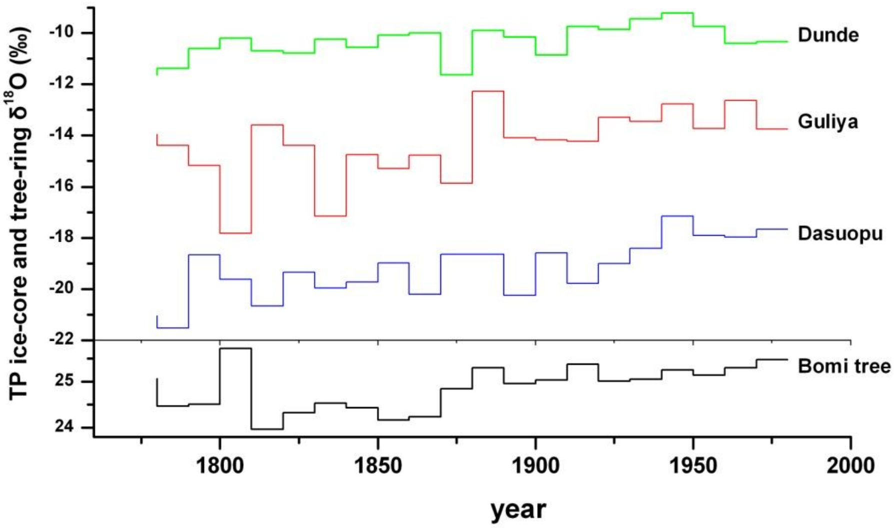

Fig. 4. Comparison of tree-ring δ^{18}O and ice-core δ^{18}O records on Tibetan Plateau (Thompson et al., 1989, 1997, 2000).

These drier conditions since the late 19th century contradict another tree-ring δ^{18}O reconstruction of annual precipitation in North Pakistan, showing that post-1850s is the wettest period of the last millennium (Treydte et al., 2006). This mismatch could be due to the different climate contexts, since the precipitation of North Pakistan is concentrated in winter and controlled by westerly flow, while Bomi precipitation mainly falls in summer and is dominated by Indian monsoon flow (Gao et al., 2010).

5 Conclusions and perspectives

A 225-yr record of tree-ring cellulose δ^{18}O is obtained for southeast TP. Based on the relationship between the tree-ring δ^{18}O and CRU cloud data derived from diurnal temperature range in the period AD 1956–2005, a summer cloud index is reconstructed, which reflects moisture variability in past 225 yr.

Our reconstruction suggests drier conditions in the 20th century than during the 19th century. The occurrence of years of extreme low or high cloud index appears to have strongly decreased since the 1920s, suggesting a relatively stable summer moisture condition in southeast TP in spite of the increasing impact of human activities on climate. The sudden increased tree-ring δ^{18}O in AD 1807–1817 reflects an exceptional decade marked by persistent dry conditions, possibly related to the impact of repeated volcanic eruptions on regional monsoon flow.

More regional tree-ring δ^{18}O records are needed to investigate the spatial changes associated with the regime shifts recorded at Bomi. Process-based understanding of the links between cloud cover and tree-ring cellulose δ^{18}O must be further investigated using atmospheric/land surface isotopic models and ecophysiological models. The tree-ring δ^{18}O data offer the potential for multi-centennial comparisons with climate model results at the regional scale.

Supplementary material related to this article is available online at: http://www.clim-past.net/8/205/2012/ cp-8-205-2012-supplement.pdf.

Acknowledgements. We thank Xiaochun Wang and Chao Zhang for the assistance of field work. The meteorological data of Bomi were obtained from the weather information centre of China Meteorological Administration. The support by the Chinese side (fieldwork, dendrochronology and data analyses) was from National Natural Science Foundation of China project No. 40631002 and the Chinese Academy of Sciences project KSCX-YW-Z-1022. The support by the French side (modelling, tree-ring stable cellulose isotopic analyses and statistical analyses) was provided by the GIS Pluies-Tibet project. The first author is grateful for the financial support by the French Embassy in China. We acknowledge Juliette Jin for the help with administration in the Chinese-French co-supervised PhD program.

Edited by: T. Kiefer

cnrs INSU Institut national des sciences de l'Univers

The publication of this article is financed by CNRS-INSU.

References

Anchukaitis, K. J., Buckley, B. M., Cook, E. R., Cook, B. I., D'Arrigo, R. D., and Ammann, C. M.: Influence of volcanic eruption son the climate of the Asia monsoon region, Geophys. Res. Lett., 37, L22703, doi:10.1029/2010GL044843, 2010.

Auer, I., Böhm, R., Jurkovic, A., Lipa, W., Orlik, A., Potzmann, R., Schöner, W., Ungersböck, M., Matulla, C., Briffa, K., Jones, P., Efthymiadis, D., Brunetti, M., Nanni, T., Maugeri, M., Mercalli, L., Mestre, O., Moisselin, J.-M., Begert, M., Müller-Westermeier, G., Kveton, V., Bochnicek, O., Stastny, P., Lapin, M., Szalai, S., Szentimrey, T., Cegnar, T., Dolinar, M., Gajic-Capka, M., Zaninovic, K., Majstorovic, Z., and Nieplova, E.: HISTALP – historical instrumental climatological surface time series of the Greater Alpine Region, Int. J. Climatol., 27, 17–46, 2007.

Barbour, M. M.: Stable oxygen isotope composition of plant tissue: a review, Funct. Plant Biol., 34, 83–94, 2007.

Bräuning, A. and Mantwill, B.: Summer temperature and summer monsoon history on the Tibetan Plateau during the last 400 years recorded by tree rings, Geophys. Res. Lett., 31, L24205, doi:10.1029/2004GL020793, 2004.

Briffa, K. R. and Osborn, T. J.: Perspectives: Climate warming – Seeing the wood from the trees, Science, 284, 926–927, 1999.

Briffa, K. R., Jones, P. D., Schweingruber, F. H., and Osborn, T. J.: Influence of volcanic eruptions on Northern Hemisphere summer temperature over the past 600 years, Nature, 393, 450–455, 1998.

Briffa, K. R., Osborn, T. J., Schweingruber, F. H., Harris, I. C., Jones, P. D., Shiyatov, S. G., and Vaganov, E. A.: Low-frequency temperature variations from a northern tree ring density network, J. Geophys. Res., 106, 2929–2941, 2001.

Cole-Dai, J., Ferris, D., Lanciki, A., Savarino, J., Baroni, M., and Thiemens, M. H.: Cold decade (AD 1810–1819) caused by Tambora and another stratospheric volcanic eruption, Geophys. Res. Lett., 36, L22703, doi:10.1029/2009GL040882, 2009.

Cook, E. R., Anchukaitis, K. J., Buckley, B. M., D'Arrigo, R. D., Jacoby, G. C., and Wright, W. E.: Asian monsoon failure and megadrought during the last millennium, Science, 328, 486–489, doi:10.1126/science.1185188, 2010.

Dai, J. H.: Volcanoes and climate, Wiley Interdisciplinary Reviews: Climate Change, 1, 824–839, 2010.

Dai, J. H., Mosley-Thompson, E., and Thompson, L. G.: Ice core evidence for an explosive tropical volcanic-eruption 6 years preceding Tambora, J. Geophys. Res., 96, 17361–17366, 1991.

Dai, A., Fung, I. Y., and Del Genio, A. D.: Surface observed global land precipitation variations during 1900–1988, J. Climate, 10, 2943–2962, 1997.

Duan, A. M. and Wu, G. X.: Change of cloud amount and the climate warming on the Tibetan Plateau, Geophys. Res. Lett., 33, L22704, doi:10.1029/2006GL027946, 2006.

Dufresne, J.-L. and Bony, S.: An assessment of the primary sources of spread of global warming estimates from coupled atmosphere-ocean models, J. Climate, 21, 5135–5144, 2008.

Esper, J., Cook, E. R., and Schweingruber, F. H.: Low-frequency signals in long tree-ring chronologies for reconstructing past temperature variability, Science, 295, 2250–2253, 2002.

Etien, N., Daux, V., Masson-Delmotte, V., Stievenard, M., Bernard, V., Durost, S., Guillemin, M. T., Mestre, O., and Pierre, M.: A bi-proxy reconstruction of Fontainebleau (France) growing season temperature from AD 1596 to 2000, Clim. Past, 4, 91–106, doi:10.5194/cp-4-91-2008, 2008.

Evans, M. N. and Schrag, D. P.: A stable isotope-based approach to tropical dendroclimatology, Geochim. Cosmochim. Ac., 68, 3295–3305, 2004.

Fan, Z. X., Bräuning, A., Yang, B., and Cao, K. F.: Tree ring density-based summer temperature reconstruction for the central Hengduan Mountains in southern China, Global Planet. Change, 65, 1–11, 2008.

Fan, F., Mann, M. E., and Ammann, C. M.: Understanding changes in the Asian summer monsoon over the past millennium: Insights from a long-term coupled model simulation, J. Climate, 22, 1736–1748, 2009.

Gao, J., Masson-Delmotte, V., Yao, T., Tian, L., Risi, C., and Hoffmann, G.: Precipitation water stable isotopes in the south Tibetan Plateau: observations and modeling, J. Climate, 24, 3161–3178, doi:10.1175/2010JCLI3736.1, 2010.

Gong, D. Y. and Luterbacher, J.: Variability of the low-level cross-equatorial jet of the western Indian Ocean since 1660 as derived from coral proxies, Geophys. Res. Lett., 35, L01705, doi:10.1029/2007GL032409, 2008.

Helliker, B. R. and Richter, S. L.: Subtropical to boreal convergence of tree-leaf temperatures, Nature, 454, 511–514, 2008.

Hilasvuori, E. and Berninger, F.: Dependence of tree ring stable isotope abundances and ring width on climate in Finnish oak, Tree. Physiol., 30, 636–647, 2010.

Holmes, R. L.: Computer-assisted quality control in tree-ring dating and measurement, Tree-Ring Bulletin, 43, 69–78, 1998.

Hourdin, F., Musat, I., Bony, S., Braconnot, P., Codron, F., Dufresne, J.-L., Fairhead, L., Filiberti, M.-A., Friedlingstein, P., Grandpeix, J.-Y., Krinner, G., LeVan, P., Li, Z.-X., and Lott, F.: The LMDZ4 general circulation model: climate performance and sensitivity to parametrized physics with emphasis on tropical convection, Clim. Dynam., 27, 787–813, 2006.

Jacobson, M. Z.: Strong radiative heating due to the mixing state of black carbon in atmospheric aerosols, Nature, 409, 695–697, 2001.

Karl, T. R., Jones, P. D., Kukla, G., Plummer, N., Razuvayev, V., Gallo, K. P., Lindseay, J., Charlson, R. J., and Peterson, T. C.: A new perspective on recent global warming – Asymmetric trends of daily maximum and minimum temperature, B. Am. Meteorol. Soc., 74, 1007–1023, 1993.

Khain, A., Rosenfeld, D., and Pokrovsky, A.: Aerosol impact on the dynamics and microphysics of deep convective clouds, Q. J. Roy. Meteor. Soc., 131, 2639–2663, 2005.

Kress, A., Saurer, M., Siegwolf, R. T. W., Frank, D. C., Esper, J., and Bugmann, H.: A 350 year drought reconstruction from Alpine tree ring stable isotopes, Global Biogeochem. Cy., 24, GB2011, doi:10.1029/2009GB003613, 2010.

Leathers, D. J., Palecki, M. A., Robinson, D. A., and Dewey, K. F.: Climatology of the daily temperature range annual cycle in the United States, Clim. Res., 9, 197–211, 1998.

Liang, E. Y., Shao, X. M., and Xu, Y.: Tree-ring evidence of recent abnormal warming on the Southeast Tibetan Plateau, Theor. Appl. Climatol., 98, 9–18, 2009.

Managave, S. R., Sheshshayee, M. S., Borgaonkar, H. P., and Ramesh, R.: Past break-monsoon conditions detectable by high resolution intra-annual delta O-18 analysis of teak rings, Geophys. Res. Lett., 37, L05702, doi:10.1029/2009GL041172, 2010.

Masson-Delmotte, V., Raffalli-Delerce, G., Danis, P. A., Yiou, P., Stievenard, M., Guibal, F., Mestre, O., Bernard, V., Goosse, H., Hoffmann, G., and Jouzel, J.: Changes in European precipitation seasonality and in drought frequencies revealed by a four-century-long tree-ring isotopic record from Brittany, western France, Clim. Dynam., 24, 57–69, 2005.

Mitchell, T. D. and Jones, P. D.: An improved method of constructing a database of monthly climate observations and associated high-resolution grids, Int. J. Climatol., 25, 693–712, 2005.

New, M., Hulme, M., and Jones, P. D.: Representing Twentieth-Century space-time climate variability. Part I: Development of a 1901–90 mean monthly terrestrial climatology, J. Climate, 12, 829–856, 1999.

New, M., Hulme, M., and Jones, P. D.: Representing Twentieth-Century space-time climate variability. Part II: Development of a 1901–96 monthly grids of terrestrial surface climate, J. Climate, 13, 2217–2238, 2000.

Oman, L., Robock, A., Stenchikov, G., Schmidt, G. A., and Ruedy, R.: Climatic response to high-latitude volcanic eruptions, J. Geophys. Res., 110, D13103, doi:10.1029/2004JD005487, 2005.

Raffalli-Delerce, G., Masson-Delmotte, V., Dupouey, J. L., Stievenard, M., Breda, N., and Moisselin, J. M.: Reconstruction of summer droughts using tree-ring cellulose isotopes: a calibration study with living oaks from Brittany (western France), Tellus, 56, 160–174, 2004.

Ramanathan, V. and Ramana, M. V.: Persistent, widespread, and strongly absorbing haze over the Himalayan foothills and the Indo-Gangetic Plains, Pure Appl. Geophys., 162, 1609–1626, 2005.

Risi, C., Bony, S., Vimeux, F., and Jouzel, J.: Water stable isotopes in the LMDZ4 General Circulation Model: model evaluation for present day and past climates and applications to climatic interpretation of tropical isotopic records, J. Geophys. Res., 115, D12118, doi:10.1029/2009JD013255, 2010.

Robock, A.: Volcanic eruptions and climate, Rev. Geophys., 38, 191–219, 2000.

Roden, J. S. and Ehleringer, J. R.: There is no temperature dependence of net biochemical fractionation of hydrogen and oxygen isotopes in tree-ring cellulose, Isot. Environ. Healt. S., 36, 303–317, 2000.

Rodionov, S. N.: A sequential algorithm for testing climate regime shifts, Geophys. Res. Lett., 31, L09204, doi:10.1029/2004GL019448, 2004.

Ruschy, D. L., Baker, D. G., and Skaggs, R. H.: Seasonal variations in daily temperature ranges, J. Climate, 4, 1211–1216, 1991.

Sano, M., Sheshshayee, M. S., Managave, S., Ramesh, R., Sukumar, R., and Sweda, T.: Climatic potential of delta O-18 of Abies spectabilis from the Nepal Himalaya, Dendrochronologia, 28, 93–98, 2010.

Schneider, D. P., Ammann, C. M., Otto-Bliesner, B. L., and Kaufman, D. S.: Climate response to large, high-latitude and low-latitude volcanic eruptions in the Community Climate System Model, J. Geophys. Res., 114, D15101, doi:10.1029/2008JD011222, 2009.

Shi, C., Masson-Delmotte, V., Daux, V., Li, Z., Zhang, Q.: An unstable tree-growth response to climate in two 500-year chronologies, North Eastern Qinghai-Tibetan Plateau, Dendrochronologia, 28, 225–237, 2010

Shi, C., Masson-Delmotte, V., Risi, C., Eglin, T., Stievenard, M., Pierre, M., Wang, X., Gao, J., Bréon, F.-M., Zhang, Q.-B., and Daux, V.: Sampling strategy and climatic implications of tree-ring stable isotopes in Southeast Tibetan Plateau, Earth. Planet. Sc. Lett., 301, 307–316, 2011.

Song, H. M., Liu, Y., Ni, W. M., Cai, Q. F., Sun, J. Y., Ge, W. B., and Xiao, W. Y.: Winter mean lowest temperature derived from tree-ring width in Jiuzhaigou region, China since 1750 AD, Quat. Sci., 27, 486–491, 2007 (in Chinese, with English abstr.).

Stephens, G. L.: Cloud feedbacks in the climate system: a critical review, J. Climate, 18, 237–273, 2005.

Sternberg, L. D. L. O.: Oxygen stable isotope ratios of tree-ring cellulose: the next phase of understanding, New Phytol., 181, 553–562, 2009.

Thompson, L. G., Mosley-Thompson, E., Davis, M. E., Bolzan, J. F., Dai, J., Yao, T., Gundestrup, N., Wu, X., Klein, L., and Xie, Z.: Holocene Late Pleistocene climatic ice core records from Qinghai-Tibetan Plateau, Science, 246, 474–477, 1989.

Thompson, L. G., Yao, T., Davis, M. E., Henderson, K. A., Mosley-Thompson, E., Lin, P. N., Beer, J., Synal, H. A., Cole-Dai, J., and Bolzan, J. F.: Tropical climate instability: The last glacial cycle from a Qinghai-Tibetan ice core, Science, 276, 1821–1825, 1997.

Thompson, L. G., Yao, T., Mosley-Thompson, E., Davis, M. E., Henderson, K. A., and Lin, P. N.: A high-resolution millennial record of the South Asian Monsoon from Himalayan ice cores, Science, 289, 1916–1919, 2000.

Treydte, K. S., Schleser, G. H., Helle, G., Frank, D. C., Winiger, M., Haug, G. H., and Esper, J.: The twentieth century was the wettest period in northern Pakistan over the past millennium, Nature, 440, 1179–1182, 2006.

Trigo, R. M., Osborn, T. J., and Corte-Real, J. M.: The North Atlantic Oscillation influence on Europe: climate impacts and associated physical mechanisms, Clim. Res., 20, 9–17, 2002.

Wang, B., Bao, Q., Hoskins, B., Wu, G., and Liu, Y.: Tibetan plateau warming and precipitation changes in East Asia, Geophys. Res. Lett., 35, L14702, doi:10.1029/2008GL034330, 2008.

Wang, W. C., Zhang, Q. Y., Easterling, D. R., and Karl, T. R.: Beijing cloudiness since 1875, J. Climate, 6, 1921–1927, 1993.

Yang, Y., Man, Z., and Zheng, Y.: A serious famine in Yunnan (1815–1817) and the eruption of Tambora Volcano, Fudan Journ., 1, 79–85, 2005 (in Chinese with English abstract).

Yao, T., Duan, K., Xu, B., Wang, N., Guo, X., and Yang, X.: Precipitation record since AD 1600 from ice cores on the central Tibetan Plateau, Clim. Past, 4, 175–180, doi:10.5194/cp-4-175-2008, 2008.

You, Q. L., Kang, S. C., Wu, Y. H., and Yan, Y. P.: Climate change over the Yarlung Zangbo river basin during 1961–2005, J. Geogr. Sci., 17, 409–420, 2007.

You, Q. L., Kang, S. C., Flugel, W. A., Sanchez-Lorenzo, A., Yan, Y. P., Huang, J., and Martin-Vide, J.: From brightening to dimming in sunshine duration over the eastern and central Tibetan Plateau (1961–2005), Theor. Appl. Climatol., 101, 445–457, 2010.

Young, G. H. F., Demmler, J. C., Gunnarson, B. E., Kirchhefer, A. J., Loader, N. J., and McCarroll, D.: Age trends in tree-ring growth and isotopic archives: a case study of *Pinus sylvestris* L. from north-western Norway, Global Biogeochem. Cy., 25, GB2020, doi:10.1029/2010GB003913, 2011.

Yu, R. C., Wang, B., and Zhou, T. J.: Climate effects of the deep continental stratus clouds generated by the Tibetan Plateau, J. Climate, 17, 2702–2713, 2004.

Zhang, X. Q., Peng, L. L., Zheng, D., and Tao, J.: Cloudiness variations over the Qinghai-Tibet Plateau during 1971–2004, J. Geogr. Sci., 18, 142–154, 2008.